

# Beam Dynamics in High Intensity Beams with Space Charge

I. Hofmann

GSI Darmstadt

P.O.B. 110552, D-64220 Darmstadt

## Abstract

For high intensity beams dominated by space charge the analysis in frequency domain and in real space and time yield complementary information on the phase space density. In the frequency domain we compare measured noise spectra of cooled heavy ion beams in the ESR with "simulation noise" obtained from computer simulation with interacting particles. This is applied to the problem of determining the phase space density from frequency measurements. As an advanced method of real space and time observation we discuss the first results of streak camera imaging of cooled heavy ion beams extracted from the ESR.

## 1 INTRODUCTION

There is a general interest to measure and optimize the longitudinal and transverse phase space density of proton or ion beams close to the limits caused by space charge effects. In storage rings proposed for heavy ion inertial fusion there is an interest to optimize the performance by pushing both the longitudinal and transverse space charge to their limits. In electron cooler rings maximum possible density in 6D phase space is an issue of general interest. It is particularly important for the challenging goal to achieve crystalline beams, where the focusing forces are exactly canceled by space charge forces.

## 2 MEASURED AND SIMULATED SCHOTTKY NOISE SPECTRA

The statistical distribution of particles gives rise to current fluctuations, which induce a voltage on a pick-up. The Schottky power spectrum is proportional to the square of the current fluctuations. For a coasting beam at low phase space density it is therefore also proportional to the momentum distribution function, since particles are completely uncorrelated in phase around the machine [1]. For high phase space density there is coherent motion in the form of waves, which leads to a strong amplification of the noise signal at the coherent frequencies (see, for example, [2, 3, 4]). For interpretation simulation is needed to bridge the gap between the simplified models of analytical theory and real beams.

In computer simulation using particles fluctuations in the density are obtained, which are analogous to the fluctuations in real beams. We have studied this in the "particle-in-cell" simulation program SCOP-RZ (Fig. 1). "Particle-in-cell" refers to the technique of calculating the electro-

magnetic interaction of the beam by creating each time-step a density function on a grid in  $r, z$  and solving Poisson's equation for an infinitely conducting pipe. Additional forces due to rf cavity impedances, kickers etc. can be included by using the measured impedance values times the Fourier component of the line density.

The longitudinal simulation Schottky noise is described by the line density, which is recorded over a large number of time steps and Fourier transformed. Smooth spectra can be obtained by averaging as in the experiment.

In Fig. 2 we show simulation noise spectra for parameters, which are typical for electron cooled beams in storage rings. The spectra have the same characteristic features as in the experiment: the left case corresponds to large uncooled momentum spread, i.e.  $\Delta p/p = 3 \times 10^{-4}$  for a 2 mA  $\text{Ne}^{10+}$  beam at 250 MeV/u; the right case to 10 times smaller cooled momentum spread. The momentum distribution is Gaussian in both cases. The two peaks for the cooled case are due to space charge waves moving with the beam velocity resp. against it. The splitting of the two peaks and the central suppression can be related to the phase space density as will be shown in the next section.

## 3 COHERENT AND INCOHERENT OSCILLATIONS

### 3.1 Longitudinal - Coasting Beam

As mentioned above coherent oscillations dominate the noise spectrum if the current is near or above the threshold of the longitudinal microwave instability given by

$$I_{thr} = \beta^2 \gamma \frac{Am_p c^2 / e}{Z} |\eta| \left( \frac{\Delta p}{p} \right)_{fwhm}^2 \left| \frac{Z_{||}}{n} \right| \quad (1)$$

Here  $Z_{||}/n$  is the total coupling impedance; for non-relativistic energies it is in general dominated by the space charge impedance  $Z_{||}/n = -i377g/(2\beta\gamma^2)$  (Ohm), with

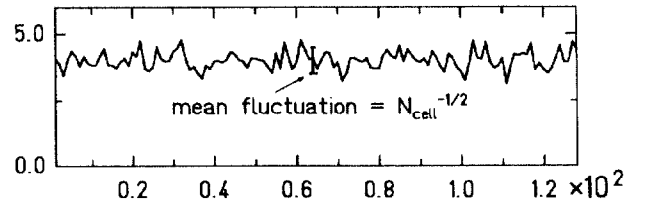


Figure 1: Fluctuations of line density in simulation of coasting beam with 8192 particles and 128 axial grid points ( $N_{cell} = 64$ ).

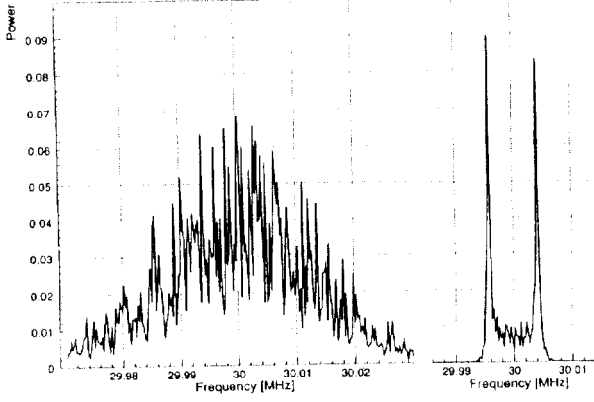


Figure 2: Simulation noise spectrum for large (left) and 10 times smaller (right) momentum spread

the geometry factor  $g = 0.5 + \ln \frac{R_p}{R_b}$  for a uniform density beam with radius  $R_b$  in a pipe of radius  $R_p$ . The above "Keil-Schnell criterion" indicates instability in very general terms for currents above the threshold and in the presence of a resistive (real) part of the impedance (below transition energy). Instability according to Eq. 1 is expected only for the special case of a quadratic momentum distribution, whereas for a Gaussian the current can considerably exceed  $I_{thr}$ . About 5–10 times higher currents have been found in storage rings with electron cooling [5, 6, 7]. It must be assumed that this is due to the enhanced Landau damping by the tails of the Gaussian momentum distribution. This question is important for heavy ion fusion storage rings, where one wants to store currents typically a factor of 10 above  $I_{thr}$  [8].

#### Beam Plasma Frequency:

The dependence of the coherent frequency shift on the momentum spread for a beam of given current can be plotted as a function of  $(\Delta p/p)^2$ . In Fig. 3 we show this dependence as calculated from the analytical dispersion relation for a Gaussian momentum distribution. We have normalized  $\Delta\omega = \omega - n\omega_0$  on the cold beam value  $(\Delta p/p = 0)$ , which is the "beam plasma frequency" given by

$$(\Delta\omega_{bp})^2 = n^2 \omega_0^2 \frac{|\eta| Z I}{2\pi\beta^2 \gamma A m c^2 / e} \left| I m \frac{Z_{||}}{n} \right| \quad (2)$$

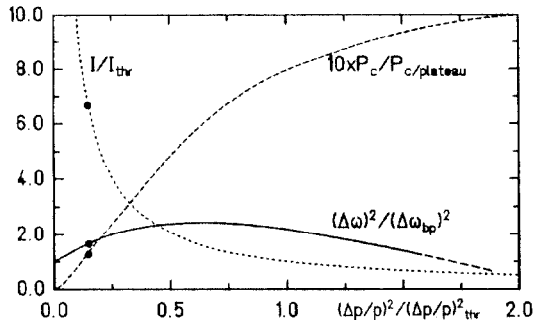


Figure 3: Normalized coherent frequency shift and  $I/I_{thr}$  vs. normalized  $(\Delta p/p)^2$  (dots r.h.s. case of Fig. 2.)

$\Delta p/p$  is normalized on  $\Delta p/p_{thr}$ , which is obtained from Eq. 1 by setting  $I = I_{thr}$ . It is noted that  $(\Delta\omega)^2$  increases linearly for small  $(\Delta p/p)^2$  to a maximum and drops again near  $(\Delta p/p)_{thr}$  when Landau damping suppresses the coherent motion. The linear increase of  $(\Delta\omega)^2$  with  $(\Delta p/p)^2$  in the beam plasma has an analogy to the dispersion relation of electron plasma waves in an infinite plasma with finite temperature [9]:

$$(\Delta\omega)^2 = \omega_p^2 + \frac{3}{2} k^2 v_{thermal}^2 \quad (3)$$

where  $k$  is the wave number,  $\omega_p^2 = e^2 n_e / (\epsilon_0 m)$  the plasma frequency squared and  $n_e$  the electron density. Hence there is a density shift corresponding to Eq. 2 as well as a temperature shift, which is actually a consequence of the plasma pressure. The derivative with respect to  $k^2$  allows to measure directly the temperature.

This is unfortunately not the case for the "beam plasma waves", where the density shift  $\Delta\omega_{bp}$  is also proportional to  $k^2 = (n/R)^2$ . Hence the graph of Fig. 3 is identical for all  $n$  (below the cut-off wavelength). This is a consequence of the electrostatic screening effect of the beam pipe for long wave lengths, i.e.  $Z_{||}/n$  is independent of  $n$ .

#### Longitudinal Phase Space Density Measurement:

The question is of interest how to determine  $I/I_{thr}$  from the Schottky spectra (i.e. without a beam transfer function measurement). It is possible to determine  $\Delta p/p$  unambiguously if we use an additional information. A reference point for evaluation is the case  $I/I_{thr} = 0.5$ , for which the Schottky spectrum has a plateau [10], which can be easily identified in the measurement. This transition from a peak in the center to a dip is also the transition of single particle to collective behaviour. For this special case the true momentum spread (fwhm) is 0.6 times the measured one. In Fig. 3 we also plot the ratio of the Schottky power at the band center ( $P_c$ ) normalized on its value for  $I/I_{thr} = 0.5$  ( $P_{c,plateau}$ ). This ratio is only a function of  $I/I_{thr}$  and independent of the precise shape of the distribution function [10]. Hence we can determine  $I/I_{thr}$  by using the graph shown in Fig. 3. With Eq. 1 the momentum spread results immediately from the corresponding value for the plateau-like spectrum according to

$$\Delta p/p = (0.5 I_{thr} / I)^{1/2} \times (\Delta p/p)_{plateau} \quad (4)$$

### 3.2 Longitudinal - Bunched Beam

For bunched beams at low intensity the direct way to determine the phase space density is a measurement of the bunch length, which is proportional to the momentum spread for a given rf potential  $V_0$ . With space charge the latter is reduced, resulting in an effective potential ("potential well flattening") and synchrotron frequency  $\omega_S$ . Here we introduce a dimensionless parameter  $\alpha$ :

$$\alpha \equiv \frac{V_0}{V_{eff}} = \frac{\omega_{S0}^2}{\omega_S^2} \quad (5)$$

$\alpha \gg 1$  indicates strongly space charge dominated bunches. We note that in heavy ion fusion storage rings  $\alpha \approx 10$  is required.

Since  $V_{eff}$  is needed to determine the momentum spread we could simply measure  $\omega_S$ . In practice this is difficult to measure on a spectrum analyzer due to the weakness of the signal. An alternative is the quadrupole mode frequency method [11]. The latter is based on the observation that the frequency of a coherent bunch length oscillation ("quadrupole mode") is closely related to the incoherent frequency shift  $\Delta\omega = \omega_{S0} - \omega_S$ . Analytical expressions exist only for the "locally elliptic" phase space distribution function, e.g.

$$f(z, \delta p/p) \propto (E - H)^{1/2} \quad (6)$$

with  $H$  the Hamiltonian. This distribution is consistent with a parabolic bunch shape [13]. The coherent oscillation frequencies of it have been calculated in Ref. [13] for the dipole (rigid displacement), quadrupole and sextupole modes as

$$\omega_1^2 = \omega_{S0}^2 \quad (7)$$

$$\omega_2^2 = 3\omega_{S0}^2 + \omega_S^2 \quad (8)$$

$$\omega_3^2 = 3\omega_{S0}^2 + 2\omega_S^2 + (9\omega_{S0}^2 + 3\omega_{S0}^2\omega_S^2 + 4\omega_S^4)^{1/2} \quad (9)$$

For small space charge shift one finds from Eq. 8 a linear relationship

$$\omega_2 - \omega_{S0} = \frac{1}{2}(\omega_{S0} - \omega_S) = \frac{\Delta\omega_S}{2} \quad (10)$$

Note that the dipole mode is not changed by space charge, which is not acting on the bunch center. The linearized relationship Eq. 10 was therefore suggested in Ref. [11] as an indirect way to determine  $\omega_S$ . For larger space charge effects the full expression of Eq. 8 was recently applied to electron cooled proton bunches leading to the conclusion that high space charge was present ( $\alpha \approx 4$ ) [12].

#### Comparison Measurement - Simulation:

Eq. 8 can be re-written in the form

$$\frac{\omega_2^2}{\omega_{S0}^2} = 3 + \frac{1}{\alpha} \quad (11)$$

The  $\alpha$ -dependent term is the space charge shift, which changes only little, if  $\alpha$  is large. Hence a small uncertainty in the quadrupole frequency results in a relatively large error in  $\alpha$ . Besides measurement errors the question arises, whether the above theoretical frequencies derived for a parabolic bunch are appropriate. Electron cooled bunches actually are known to be Gaussian in shape rather than parabolic (see also section 4).

In order to investigate possible ambiguities we have directly measured  $\omega_2$  as well as  $\omega_S$  and  $\omega_{S0}$  for  $\text{Ne}^{10+}$  bunches in the ESR storage ring at an energy of 250 MeV/u. A typical example of the Schottky spectrum of a cooled bunch with  $3 \times 10^8$  particles and an rf voltage of 100 V is shown in Fig. 4 (Ref. [14]).

Besides synchrotron satellites we have multiples of 50 Hz, which are presumably due to electronic coupling. Due to space charge each sideband is split into several lines for coherent and incoherent frequencies. In order to increase the confidence in interpreting individual lines we

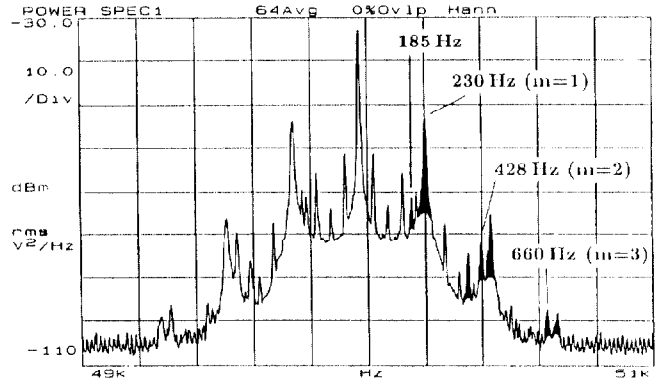


Figure 4: Measured Schottky spectrum for bunched beam with space charge effects (relevant satellites filled black).

have also calculated the computer simulation noise. Results are shown in Fig. 5 for the same parameters as in Fig. 4. The simulation shows the same splitting as the experiment. The height of sidebands is expected to differ, depending on the initial excitation. Relevant frequencies in Fig. 4 are  $\omega_{S0} = 230$  Hz,  $\omega_S = 185$  Hz (as well as twice these frequencies),  $\omega_2 = 428$  Hz.

From Eq. 5 we calculate  $\alpha$  as 1.6 in this example, hence 40% of the applied rf voltage is compensated by space charge.

The findings from experiment, simulation noise and the above analytical formulae are compared in Fig. 6. The agreement between analytical theory and simulation noise with the distribution function of Eq 6 is excellent. The measured  $\omega_2$  values are, however, systematically lower than the calculated ones. If we had used Eq. 11,  $\alpha$  would have resulted nearly 40–50% larger than the true value. The uncertainty might even increase at larger values of  $\alpha$ . A possible direction to explain this is a different longitudinal phase space distribution in the real beam. This is confirmed in section 4, where a Maxwellian is suggested.

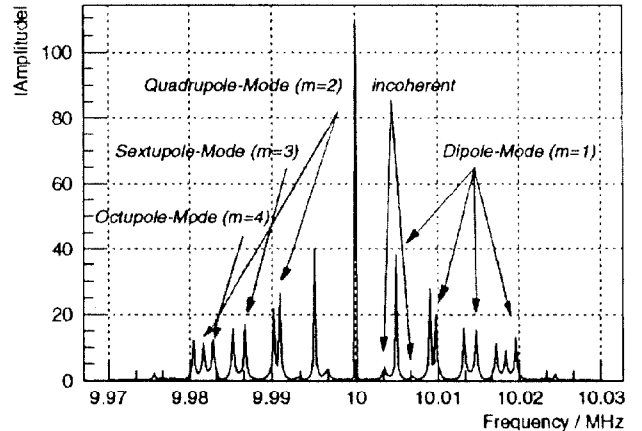


Figure 5: Simulation noise for parameters of Fig. 4.

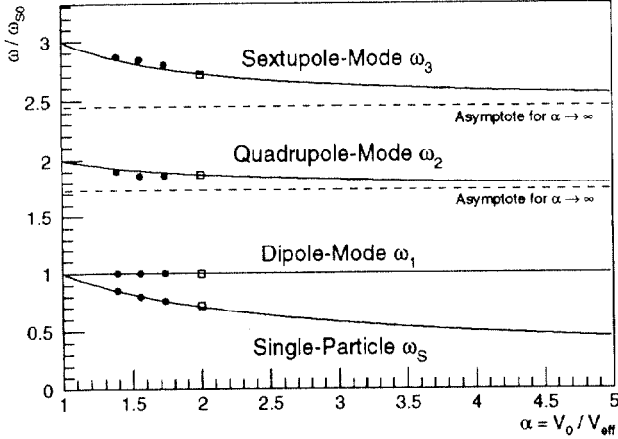


Figure 6: Comparison of space charge effects on longitudinal bunch spectrum between experiment (dots), simulation noise (squares) and analytical formulae (lines).

### 3.3 Transverse Phase Space Density

As in the longitudinal case, a direct measurement of the incoherent tune shift is difficult due to the weak signals. One can try to measure again a coherent quadrupole oscillation frequency shift, which also reflects the space charge density. In a round cross section beam (with symmetric focusing strength) there are two such "envelope" modes": a "breathing mode" leaving the beam symmetric and an antisymmetric "deformation mode" leaving the density unchanged. For this special case one easily finds from the KV - envelope equations simple expressions for the quadrupole mode tunes in terms of the incoherent tune shift  $\Delta Q_{inc}$ :

$$\Delta Q_{2,s} = 2 Q_0 - \frac{3}{2} \Delta Q_{inc} \quad (12)$$

$$\Delta Q_{2,a} = 2 Q_0 - \Delta Q_{inc} \quad (13)$$

It should be noted here that in the absence of space charge the quadrupole tunes are simply  $2 Q_0$ . More generally the tune shifts are calculated numerically from the KV - envelope equations. As an example we show in Fig. 7 a calculation for different horizontal tunes and emittances:  $Q_{0,h} = 4.29$ ,  $Q_{0,e} = 3.29$ ,  $\epsilon_h = 200\pi$ ,  $\epsilon_e = 50\pi$ . The measurement requires an appropriate pickup to detect the oscillation. While the dipole frequency (unaffected by space charge) is measured by the difference signal of two opposite

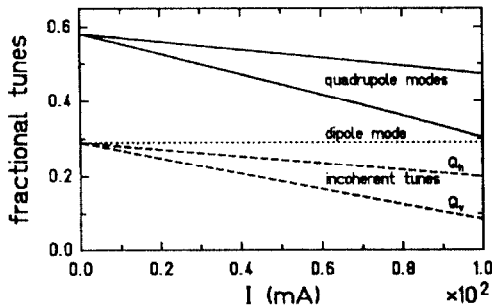


Figure 7: Quadrupole tune shifts for different emittances.

plates, the quadrupole mode requires the difference signal of two plates  $90^\circ$  apart. Contrary to the dipole mode the signal decays strongly with the distance from the beam.

## 4 3-D DIAGNOSTICS

For high-current beam dynamics studies we have implemented a streak camera as a new method of diagnostics in the environment of an ion beam storage ring. The narrow slit of the streak camera is directed on a fast plastic scintillator, which is hit by the beam in the reinjection line between the ESR and SIS. The streaking of the image allows to represent the horizontal density profile vs. time at a resolution of about 2 ns. Quantitative evaluation requires to avoid saturation of the scintillator by creating large enough spots (see also Ref. [15]). This diagnostic thus allows measurements simultaneously in time and in either horizontal or vertical direction.

### 4.1 Stationary Bunches in Cooling Equilibrium

Measurements are shown here for  $C^{6+}$  bunches (harmonic 2) at 250 MeV/u in equilibrium with the electron cooling for a circulating ion current of 0.13 mA. The horizontal beam profile at the bunch center as well as the time profile along the main axis of the bunch have been determined to be close to Gaussian. Results are shown in Fig. 8, where the data are fit with a Gaussian plus a constant background. At times and positions other than those of the bunch center, the time and position profiles are also Gaussian.

#### 3-D Equilibrium Distribution:

Evaluation of horizontal profiles at different times allows to determine the horizontal emittance along the bunch (in absolute units, if the beta-function is determined at the scintillator). We found that the bunch size resp. emittance is constant along the bunch (Fig. 9). With the Gaussian bunch current profile this result is fundamentally different from the coasting beam scaling for intrabeam scattering,  $\epsilon \propto I^a$ , with  $a \approx 0.5$  [16]. The reason for this should be seen in the synchrotron motion, which moves particles

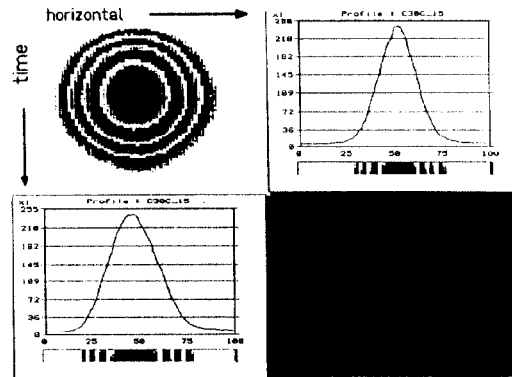


Figure 8: Streak camera image of  $C^{6+}$  bunch with time profile and horizontal profile through bunch center.

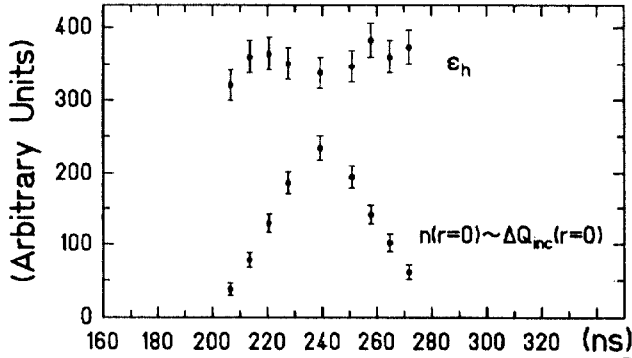


Figure 9: Measured emittance and space charge tune shift vs. time for bunch of Fig. 8.

throughout the bunch in a time, which is short compared with the scattering time.

The Gaussian densities and constant emittance suggest to use a "two-temperature" Maxwellian distribution to describe the bunches in equilibrium with electron cooling, i.e.

$$f \propto \exp(-H_{\parallel}/kT_{\parallel}) \times \exp(-H_{\perp}/kT_{\perp}) \quad (14)$$

with decoupled Hamiltonians for the parallel ( $z$ ) and transverse phase space, and with independent temperatures. The Maxwellian has temperatures independent from positions, which is equivalent to constant angular spread (hence emittance) and momentum spread. Densities are Gaussian as long as the potentials are harmonic, or near harmonic ( $\alpha$  not too large).

#### Space Charge Tune Shift:

The bunch current and horizontal and vertical rms sizes resolved along the bunch can be used to calculate the incoherent tune shifts along the bunch. For a round beam the density measurement on the bunch axis gives directly the variation of the incoherent tune shift for small betatron amplitudes due to

$$\Delta Q_{inc}^{(r=0)} \propto \frac{d}{dr} E_r(r=0, z) \propto n(r=0, z) \quad (15)$$

The assumption of roundness (in the time average) is approximately satisfied for electron cooled bunches, hence Eq. 15 is applicable (Fig. 9).

#### 4.2 Instability Studies

The relevance of streak camera observation for bunch instabilities is shown in the following example. For circulating currents exceeding approximately 2 mA (i.e. more than 10 mA peak currents) it was observed that the bunches are periodically unstable. On the DSA a double-humped, broadened bunch profile was observed. After typically a second of cooling sharp bunch profiles were re-established and quickly broadened, and so on. In Fig. 10 a streak image is shown for a bunch extracted in the middle of an unstable phase. The observation of simultaneous blow-up of momentum spread and emittance suggests that the cooling mechanism plays an important role in driving the instability. We assume that the variation of the ion beam space

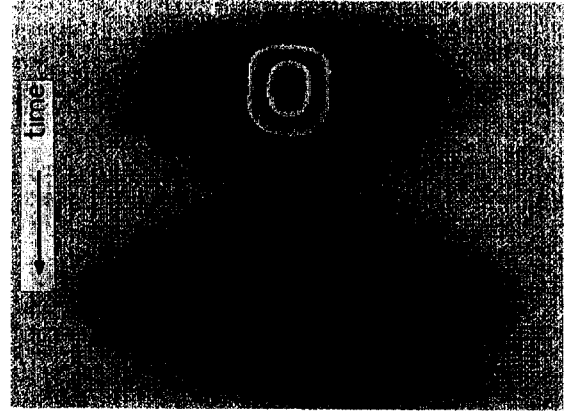


Figure 10: Unstable phase of intense bunches (harmonic 2) with electron cooling showing equidensity contours.

charge along the bunch leads to a variation of the electron cooler energy and thus a dynamical mismatch between rf frequency and electron velocities. Quantitatively we find approximately 0.5 Volts of energy change per mA of ion current. This is equivalent to a shift of  $\Delta p/p$  of  $2 \times 10^{-5}$ , by which the optimum of electron cooling is pushed away from the bunch center. It remains to be clarified whether other destabilizing mechanisms contribute also to this observation.

**Acknowledgment:** The author would like to thank his colleagues in the Plasma Physics group and the ESR group at GSI for their support in the measurements.

#### 5 REFERENCES

- 1 J. Borer et al., Proc. IXth Conf. on High Energy Accelerators, Stanford, 1974, p.53
- 2 V. Parkhomchuk and D. Pestrikov, "Thermal noise in an intense beam in a storage ring", Sov. Phys. Tech. Phys. 25(7), p.818 (1980)
- 3 E.N. Dementev et al., Sov. Phys. Tech. Phys. 25(8), 1001 (1980)
- 4 S. Cocher and I. Hofmann, Part. Accel. 34, 189 (1990)
- 5 P. Baumann et al., Nucl. Instr. and Meth. A 268, 531 (1988)
- 6 J. Bossert et al., Proc. Part. Acc. Conf., San Francisco, May 6-9, 1991, p. 2509 (1991)
- 7 I. Hofmann, Proc. Part. Acc. Conf., San Francisco, May 6-9, 1991, p. 2492 (1991)
- 8 I. Hofmann, Nuovo Cimento 106 A, 1445(1993)
- 9 D. Bohm and E.P. Gross, Phys. Rev. 75, 1851, 1864 (1949)
- 10 I. Hofmann, K. Beckert, S. Baumann-Cocher and U. Schaaf, Proc. European Part. Accel. Conf., Nice, June 12-14, 1990, p.229
- 11 S. Hansen et al., IEEE Trans. Nucl. Sci. NS-22, 1381 (1975)
- 12 S.S. Nagaitsev et al., Proc. Workshop on Beam Cooling and Related Topics, Montreux, 4-8 October, 1993, p.405
- 13 D. Neuffer, LBL-preprint 9605 (1979)
- 14 G. Kalisch, Dissertation, GSI-Report 94-05 (1994)
- 15 K. Johnson et al., these proceedings
- 16 M. Steck et al., Proc. Workshop on Beam Cooling and Related Topics, Montreux, 4-8 October, 1993, p.395